A Screw Theory Based Approach to Determining the Identifiable Parameters for Calibration of Parallel Manipulators

F. W. Yin [a], W. J. Tian [b], H. T. Liu [a], T. Huang [a,c,*] , and D. G. Chetwynd[c]

[a]Key laboratory of Modern Mechanisms and Equipment Design of Education Ministry, Tianjin University, Tianjin 300072, China
[b]School of Marine Science and Technology, Tianjin University, Tianjin 300072, China
[c]School of Engineering, The University of Warwick, Coventry CV4 7AL, UK

Abstract: Establishing complete, continuous and minimal error models is fundamentally significant for the calibration of robotic manipulators. Motivated by practical needs for models suited to coarse plus fine calibration strategies, this paper presents a screw theory based approach to determining the identifiable geometric errors of parallel manipulators at the model level. The paper first addresses two specific issues: (1) developing a simple approach that enables all encoder offsets to be retained in the minimal error model of serial kinematic chains; and (2) exploiting a fully justifiable criterion that allows the detection of the unidentifiable structural errors of parallel manipulators. Merging these two threads leads to a new, more rigorous formula for calculating precisely the number of identifiable geometric errors, including both encoder offsets and identifiable structural errors, of parallel manipulators. It shows that the identifiability of structural errors in parallel manipulators depends highly upon joint geometry and actuator arrangement of the limb involved. The process is used to determine the unidentifiable structural errors of two lower mobility parallel mechanisms to illustrate the effectiveness of the proposed approach.

Keyword: Robotic manipulators, Error modeling, Calibration, Identifiability

1. Introduction

Geometric accuracy is a crucially important performance factor for parallel kinematic machines, especially those developed for 5-axis NC machining and precision assembly, where relatively high pose accuracy is a major requirement. Kinematic calibration by software is recognized as a practical and economical way to improve pose accuracy if sufficient repeatability can be ensured by means of tolerance design, manufacturing and assembly processes. Calibration essentially requires a complete, continuous and minimal model that relates the predicted pose error twist of the end-effector to the corrections that are to be applied to the current kinematic parameters, generally by iterative least squares [1–4].

Over the past decades, there has been a great deal of intensive research into geometric error modeling of serial manipulators. There are two ways to formulate error models for calibration. The first way is to take small perturbation of the forward kinematics represented by a sequence of homogeneous transformation matrices built by the D-H (Denavit–Hartenberg) convention [5,6]. Various modified versions have been published for dealing with the parametric discontinuities arising with nearly parallel neighboring axes and/or the arbitrary localization of a tool frame attached to the end-effector [2,7–14]. The second way uses differentiation of the forward kinematics represented by the POE (Product of Exponentials) formulae [15–26], which can be established in either the global or local sense, depending upon the frames in which the joint twist coordinates are evaluated. Several methods have been proposed within each of these methods for determining the identifiable parameters *via* redundancy elimination at the model level [11–14,20–26]. A feature common to both D-H and POE based methods is that the encoder offset of a prismatic joint has to be treated as the redundant error parameter that must thereby be removed from the error model. A straightforward explanation of this result is that the twist axis of a prismatic joint is a free vector so that it only needs two angular parameters to describe the direction [11,12,22–25]. In addition, singular value decomposition (SVD) is an alternative way for determining the identifiable parameters at the calibration level [26–36]. Although a column full ranked identification Jacobian can be guaranteed, the retained error parameters have no longer geometrical meanings. However, the pose errors caused by the encoder offsets are usually much larger than those caused by the structural errors of joints and links. The preferable practice is to coarsely identify and compensate the encoder offsets iteratively until they are reduced below the level at which the linearized model becomes valid for full parameter identification and pose error compensation. Therefore, it is essential to develop an approach that enables all encoder offsets to be retained in the error model under the requirements of completeness, continuity and minimality for calibration.

Because of the complicated topological structures of parallel manipulators, there has been little work on determining their identifiable error parameters at the model level [37–40], although great efforts have been made at the calibration level using singular value decomposition [28–36]. For example, an empirical formula $\sum_{i=1}^{l}\left(3n_{r,i}+n_{p,i}+n_{ss,i}\right)+6$ was proposed [37] where $n_{r,i}$ and $n_{p,i}$ denote the number of revolute and prismatic joints and $n_{ss,i}$ the number of links between two spherical joints in limb i ($i=1,2,\ldots,l$) with l being the number of limbs of a parallel manipulator. This formula was then amended to take account of the number of independent loop closures and the number of cylindrical joints involved [38,39]. Unfortunately, as remarked by [40], these formulae were tested only *via* case-by-case studies without any formal justifiable proof. More recently, an interesting attempt to use the POE based approach [40] for dealing with the same problem provided a formula $\sum_{i=1}^{l}\left(4n_{r,i}+2n_{p,i}\right)+6=4n_r+2n_p+6$ that can be used to count the maximal number of identifiable parameters of non-overconstrained and non-redundantly actuated parallel manipulators. This formula has exactly the same form as that for serial manipulators. The formula was claimed to be independent of the topological structure of a parallel manipulator in terms of joint geometry and actuation arrangement. Although this formula can be derived with ease by the G-K mobility criterion, its validity is indeed debatable because a structural error might be intrinsically unidentifiable, a criticism justified in this article.

Driven by the practical needs for a coarse plus fine calibration strategy, this paper presents a screw theory based approach to determining the identifiable geometric errors for the calibration of parallel manipulators. Its particular goal is to exploit a justifiable criterion that allows both redundant and unidentifiable structural error parameters to be detected while retaining all encoder offsets in the minimal error model. After this brief review of the major challenges, Section 2 first formulates the linearized error model of a serial kinematic chain based upon the modified D-H convention [7]. Then, it proposes a simple method that enables the encoder offsets to be retained in the established minimal error model by linear correlation analysis of a set of unit twists associated with the axes of three consecutive body-fixed frames. Section 3 starts by formulating a linearized error model of parallel manipulators by using the dual and reciprocal properties of wrench and twist systems of the platform. Exploration follows a criterion that enables unidentifiable structural errors within a limb to be detected by examining the virtual work done by the unit wrenches that the limb imposes on the unit twist associated with the structural error being considered. Merging the ideas developed in Sections 2 and 3 results in a new formula that calculates precisely the number of identifiable error parameters of parallel manipulators. The effectiveness of the proposed method is illustrated in Section 4 *via* dealing with two lower mobility parallel mechanisms before conclusions are drawn in Section 5.

2. Minimal Error Model of Serial Kinematic Chains

2.1 Error modeling

Fig.1 shows the schematic diagram of a serial kinematic chain composed of a base and *n* movable links serially connected by *n* 1-DOF actuated joints. In order to avoid parametric discontinuities arising when two consecutive joints have nearly parallel axes, we establish the following frames using the modified D-H convention [7].

(1) Global reference frame K_0 attached to the base (link 0);

(2) Body frames K_{j+1} ($j=0,1,\ldots,n-1$) attached to link j with the z_{j+1} axis aligned with the $(j+1)$th joint axis;

(3) Body frames K_{n+1} and K_{n+2} attached to link n with the z_{n+2} axis aligned with the tool axis of the end-effector and its origin located at the tool tip point (TCP);

(4) Intermediate frames $\bar{K}_j$ ($j=1,2,\ldots,n+1$) attached to link j with the origin coincident with that of K_j and the $\bar{y}_j$ axis aligned with the y_j axis as shown in Fig.2;

(5) Moving global reference frame K_0' with its origin nominally coincident with the TCP and its axes remaining parallel to those of K_0.

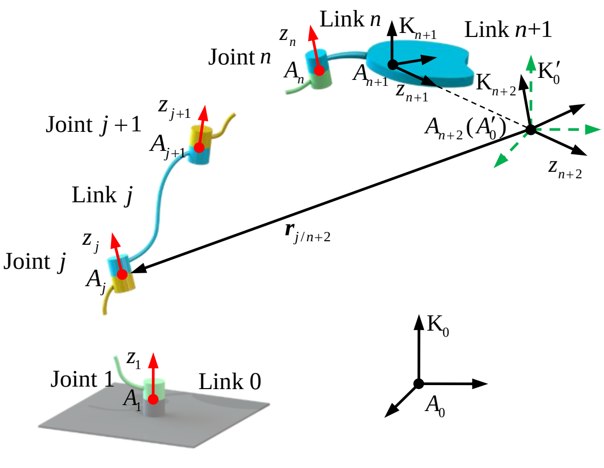

Fig. 1 The Schematic diagram of a serial kinematic chain, with link *n* being the platform and link *n*+1 the tool.

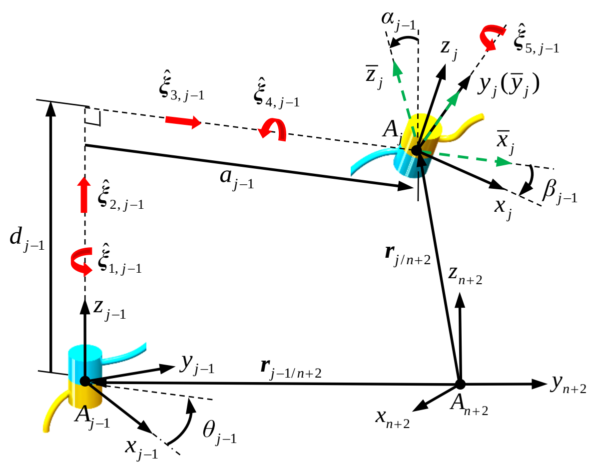

Fig. 2 The additional parameter β_{j-1} about the y_j axis is employed.

A_j represents the origin of K_j $(j=0,1,2,\cdots,n+2)$ as shown in Fig.1. Consequently, the homogeneous transformation matrix of K_j with respect to K_{j-1} $(j=1,2,\cdots,n+1)$ can be consistently parameterized by θ_{j-1}, d_{j-1}, a_{j-1}, α_{j-1} and β_{j-1}. Here, θ_{j-1} denotes the angle from x_{j-1} to x_j measured about z_{j-1}; d_{j-1} the distance from x_{j-1} to $\bar{x}_j$ measured along z_{j-1}; a_{j-1} the distance from z_{j-1} to $\bar{z}_j$ measured along $\bar{x}_j$; α_{j-1} the angle from z_{j-1} to $\bar{z}_j$ measured about $\bar{x}_j$; and β_{j-1} the angle from $\bar{x}_j$ to x_j measured about $\bar{y}_j$. Note that the nominal value of β_{j-1} is set to be zero because ideally $\bar{K}_j$ is aligned with K_j; its deviation represents particular misalignment about the $\bar{y}_j$ axis as clearly depicted in Fig.2. In addition, we use the first two D-H parameters, θ_{n+1} and d_{n+1}, to describe the transformation between K_{n+2} and K_{n+1}. Hence, the pose (position and orientation) of the end-effector can be expressed by successive 4×4 homogeneous transformations

$$
{}^{0}\boldsymbol{T}_{n+2}=\prod_{j=1}^{n+1}\prod_{k=1}^{5}\boldsymbol{T}_{k,j-1}\prod_{k=1}^{2}\boldsymbol{T}_{k,n+1} \tag{1}
$$

$$
\boldsymbol{T}_{1,j-1}=\mathrm{Rot}\left(z_{j-1},\theta_{j-1}\right),\quad \boldsymbol{T}_{2,j-1}=\mathrm{Trans}\left(z_{j-1},d_{j-1}\right),\quad \boldsymbol{T}_{3,j-1}=\mathrm{Trans}\left(\bar{x}_j,a_{j-1}\right)
$$

$$
\boldsymbol{T}_{4,j-1}=\mathrm{Rot}\left(\bar{x}_j,\alpha_{j-1}\right),\quad \boldsymbol{T}_{5,j-1}=\mathrm{Rot}\left(\bar{y}_j,\beta_{j-1}\right),\quad j=1,2,\cdots,n+1
$$

$$
\boldsymbol{T}_{1,n+1}=\mathrm{Rot}\left(z_{n+1},\theta_{n+1}\right),\ \boldsymbol{T}_{2,n+1}=\mathrm{Trans}\left(z_{n+1},d_{n+1}\right)
$$

Assume that the structural errors are much smaller than the relevant nominal parameters and all the encoder errors have been reduced below the level at which the linearized model becomes valid by means of the coarse calibration. These conditions allows the linearized error model of the serial kinematic chain to be formulated by taking small perturbation on both sides of Eq.(1), ignoring higher-order terms in the deviations of kinematic parameters, and applying appropriate isomorphism transformations.

$$
\boldsymbol{\xi}=\sum_{j=1}^{n+1}\sum_{k=1}^{5}\eta_{k,j-1}\hat{\boldsymbol{\xi}}_{k,j-1}+\sum_{k=1}^{2}\eta_{k,n+1}\hat{\boldsymbol{\xi}}_{k,n+1} \tag{2}
$$

$$
\hat{\boldsymbol{\xi}}_{1,j-1}=\begin{pmatrix}\boldsymbol{r}_{j-1/n+2}\times\boldsymbol{w}_{j-1}\\ \boldsymbol{w}_{j-1}\end{pmatrix},\ \hat{\boldsymbol{\xi}}_{2,j-1}=\begin{pmatrix}\boldsymbol{w}_{j-1}\\ \boldsymbol{0}\end{pmatrix},\ \hat{\boldsymbol{\xi}}_{3,j-1}=\begin{pmatrix}\boldsymbol{u}_{j}\\ \boldsymbol{0}\end{pmatrix},\ \hat{\boldsymbol{\xi}}_{4,j-1}=\begin{pmatrix}\boldsymbol{r}_{j/n+2}\times\boldsymbol{u}_{j}\\ \boldsymbol{u}_{j}\end{pmatrix},\ \hat{\boldsymbol{\xi}}_{5,j-1}=\begin{pmatrix}\boldsymbol{r}_{j/n+2}\times\boldsymbol{v}_{j}\\ \boldsymbol{v}_{j}\end{pmatrix}
$$

$$
\eta_{1,j-1}=\delta\theta_{j-1},\ \eta_{2,j-1}=\delta d_{j-1},\ \eta_{3,j-1}=\delta a_{j-1},\ \eta_{4,j-1}=\delta\alpha_{j-1},\ \eta_{5,j-1}=\delta\beta_{j-1},\ \boldsymbol{w}_{j-1}\perp\boldsymbol{u}_{j},\ j=1,2,\cdots,n+1
$$

$$
\hat{\boldsymbol{\xi}}_{1,n+1}=\begin{pmatrix}\boldsymbol{r}_{n+1/n+2}\times\boldsymbol{w}_{n+1}\\ \boldsymbol{w}_{n+1}\end{pmatrix},\ \hat{\boldsymbol{\xi}}_{2,n+1}=\begin{pmatrix}\boldsymbol{w}_{n+1}\\ \boldsymbol{0}\end{pmatrix},\ \eta_{1,n+1}=\delta\theta_{n+1},\ \eta_{2,n+1}=\delta d_{n+1}
$$

where $\boldsymbol{\xi}$ denotes the error twist about A_{n+2}; $\hat{\boldsymbol{\xi}}_{k,j-1}$ $(k=1,2,\cdots,5)$ denotes the unit twist of the relevant frame's axis along/about which the kth geometric error $\eta_{k,j-1}$ of K_j with respect to K_{j-1} is defined; $\boldsymbol{r}_{j-1/n+2}$ ($\boldsymbol{r}_{j/n+2}$) denotes the nominal vector pointing from A_{n+2} to A_{j-1} (A_j). $\boldsymbol{w}_{j-1}$, $\boldsymbol{u}_j$ and $\boldsymbol{v}_j$ are the nominal unit vectors of the z_{j-1}, x_j and y_j axes, respectively; in the linear, first order model x_j and $\bar{x}_j$ are functionally indistinguishable.

2.2 Elimination of redundant error parameters

We now present a simple method to determine the redundant error parameters such that the encoder offsets can be retained in the minimal error model. In order to do so, evaluate in K_{j+1} $(j=1,2,\cdots,n+1)$ twelve unit twists corresponding to the axes of three consecutive frames K_{j-1}, K_j and K_{j+1}. It is worthwhile pointing out that this treatment differs from the previous works [12,24–27] where linear correlation among six unit twists associated with two consecutive frames were merely analyzed such that the encoder offset of a prismatic joint has to be treated as a redundant term, it thereby must be removed. The left superscript indicates the frame in which the Plücker coordinates of a unit twist are expressed. Evaluated in K_{j+1}, the positioning vectors pointing from A_{j+1} to A_{j-1} and A_j can be expressed as

$$
{}^{j+1}\boldsymbol{r}_{j-1/j+1}=-a_j\hat{\boldsymbol{x}}-d_j\,{}^{j+1}\boldsymbol{w}_j-a_{j-1}{}^{j+1}\boldsymbol{u}_j-d_{j-1}{}^{j+1}\boldsymbol{w}_{j-1},\quad {}^{j+1}\boldsymbol{r}_{j/j+1}=-a_j\hat{\boldsymbol{x}}-d_j\,{}^{j+1}\boldsymbol{w}_j \tag{3}
$$

$$
\hat{\boldsymbol{x}}=\begin{pmatrix}1&0&0\end{pmatrix}^{\mathrm{T}},\ \hat{\boldsymbol{y}}=\begin{pmatrix}0&1&0\end{pmatrix}^{\mathrm{T}},\ \hat{\boldsymbol{z}}=\begin{pmatrix}0&0&1\end{pmatrix}^{\mathrm{T}}
$$

This allows ${}^{j+1}\hat{\boldsymbol{\xi}}_{k,j-1}$ $(k=1,2,\cdots,5)$, ${}^{j+1}\hat{\boldsymbol{\xi}}_{k,j}$ $(k=1,2,\cdots,5)$ and ${}^{j+1}\hat{\boldsymbol{\xi}}_{k,j+1}$ $(k=1,2)$ about A_{j+1} to be expressed as

$$
{}^{j+1}\hat{\xi}_{1,j-1}=\begin{pmatrix}\left(-a_j\hat{\boldsymbol{x}}-d_j\,{}^{j+1}\boldsymbol{w}_j-a_{j-1}\,{}^{j+1}\boldsymbol{u}_j\right)\times{}^{j+1}\boldsymbol{w}_{j-1}\\ {}^{j+1}\boldsymbol{w}_{j-1}\end{pmatrix},\quad {}^{j+1}\hat{\xi}_{2,j-1}=\begin{pmatrix}{}^{j+1}\boldsymbol{w}_{j-1}\\ \boldsymbol{0}\end{pmatrix},\quad {}^{j+1}\hat{\xi}_{3,j-1}=\begin{pmatrix}{}^{j+1}\boldsymbol{u}_{j}\\ \boldsymbol{0}\end{pmatrix}
$$
$$
{}^{j+1}\hat{\xi}_{4,j-1}=\begin{pmatrix}\left(-a_j\hat{\boldsymbol{x}}-d_j\,{}^{j+1}\boldsymbol{w}_j\right)\times{}^{j+1}\boldsymbol{u}_{j}\\ {}^{j+1}\boldsymbol{u}_{j}\end{pmatrix},\quad {}^{j+1}\hat{\xi}_{5,j-1}=\begin{pmatrix}\left(-a_j\hat{\boldsymbol{x}}-d_j\,{}^{j+1}\boldsymbol{w}_j\right)\times{}^{j+1}\boldsymbol{v}_{j}\\ {}^{j+1}\boldsymbol{v}_{j}\end{pmatrix}
$$
$$
{}^{j+1}\hat{\xi}_{1,j}=\begin{pmatrix}-a_j\hat{\boldsymbol{x}}\times{}^{j+1}\boldsymbol{w}_j\\ {}^{j+1}\boldsymbol{w}_j\end{pmatrix},\quad {}^{j+1}\hat{\xi}_{2,j}=\begin{pmatrix}{}^{j+1}\boldsymbol{w}_j\\ \boldsymbol{0}\end{pmatrix},\quad {}^{j+1}\hat{\xi}_{3,j}=\begin{pmatrix}\hat{\boldsymbol{x}}\\ \boldsymbol{0}\end{pmatrix},\quad {}^{j+1}\hat{\xi}_{4,j}=\begin{pmatrix}\boldsymbol{0}\\ \hat{\boldsymbol{x}}\end{pmatrix},\quad {}^{j+1}\hat{\xi}_{5,j}=\begin{pmatrix}\boldsymbol{0}\\ \hat{\boldsymbol{y}}\end{pmatrix}
$$
$$
{}^{j+1}\hat{\xi}_{1,j+1}=\begin{pmatrix}\boldsymbol{0}\\ \hat{\boldsymbol{z}}\end{pmatrix},\quad {}^{j+1}\hat{\xi}_{2,j+1}=\begin{pmatrix}\hat{\boldsymbol{z}}\\ \boldsymbol{0}\end{pmatrix} \tag{4}
$$

with

$$
{}^{j+1}\boldsymbol{R}_j=\left[{}^{j+1}\boldsymbol{u}_j\quad {}^{j+1}\boldsymbol{v}_j\quad {}^{j+1}\boldsymbol{w}_j\right],\quad {}^{j+1}\boldsymbol{w}_{j-1}={}^{j+1}\boldsymbol{R}_j\,{}^{j}\boldsymbol{w}_{j-1},\quad {}^{j}\boldsymbol{w}_{j-1}=\left(0\quad \sin\alpha_{j-1}\quad \cos\alpha_{j-1}\right)^{\mathrm{T}}
$$

where ${}^{j+1}\boldsymbol{R}_j$ denotes the orientation matrix of K_{j+1} with respect to K_j.

Examining Eq.(4) indicates that: (a) ${}^{j+1}\hat{\xi}_{k,j}(k=3,4,5)$ and ${}^{j+1}\hat{\xi}_{k,j+1}(k=1,2)$ are always constant unit twists; (b) if joint j is prismatic ${}^{j+1}\boldsymbol{R}_j$ becomes a constant matrix, leading to ${}^{j+1}\hat{\xi}_{k,j-1}(k=2,3)$ and ${}^{j+1}\hat{\xi}_{k,j}(k=1,2)$ being constant unit twists; and (c) ${}^{j+1}\hat{\xi}_{1,j-1}$ becomes a constant unit twist if joint j is prismatic and z_j is parallel to z_{j-1}. Recalling that the β parameter was introduced to deal with singular geometries, $\eta_{5,j-1}$ and $\eta_{5,j}$ are redundant unless specific parallel conditions apply, in which case an alternative parameter must be taken instead. Building upon these observations, we propose a simple method for determining the redundant error parameters by considering the following two cases.

Case 1: When joint j is revolute, $\eta_{2,j}$ is a structural error and there are two redundant parameters. If z_j is parallel to z_{j+1} (z_{j-1}), retain $\eta_{5,j}$ ($\eta_{5,j-1}$) and take $\eta_{2,j}$ as the redundant error parameter because it can be merged into $\eta_{2,j+1}$ ($\eta_{2,j-1}$). Otherwise, take $\eta_{5,j}$ ($\eta_{5,j-1}$) as a redundant error parameter in accordance with the basic D-H convention.

Case 2: When joint j is prismatic, $\eta_{2,j}$ becomes an encoder offset that must be retained. Two steps are needed to determine the four redundant error parameters.

Step 1: If z_j is parallel to z_{j+1} (z_{j-1}), retain $\eta_{5,j}$ ($\eta_{5,j-1}$) and take $\eta_{2,j+1}$ ($\eta_{2,j-1}$) as the redundant error parameter as it can be merged into $\eta_{2,j}$. Otherwise, take $\eta_{5,j}$ ($\eta_{5,j-1}$) as the redundant error parameter according to the basic D-H convention.

Step 2: Take $\eta_{3,j-1}$ and $\eta_{3,j}$ as always redundant error parameters as a consequence of the linear correlation analysis of the constant unit twists.

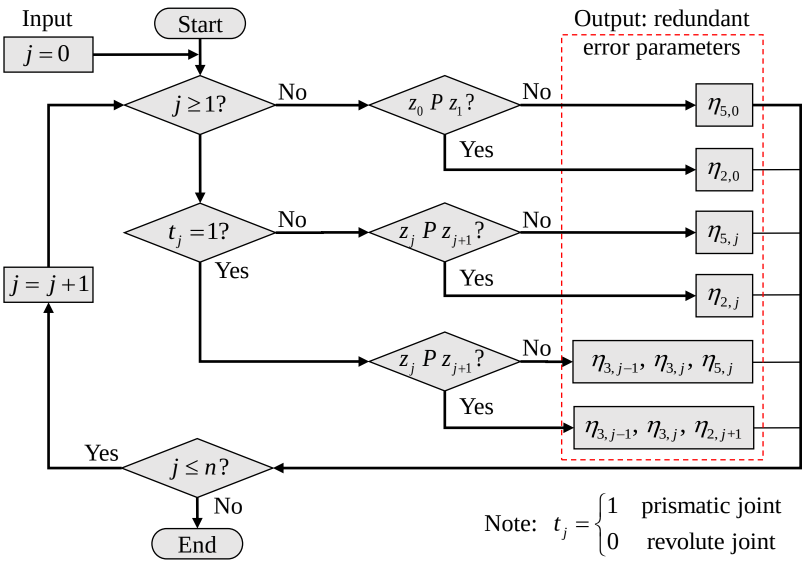

Fig. 3 The forward algorithm for determining the redundant error parameters

This redundancy elimination procedure can be implemented by either a forward or a backward algorithm throughout the entire chain, i.e. from the base to the end-link or vice versa. Fig.3 shows the flow chart of the forward algorithm. It is important to note that some of the redundant error parameters determined by the forward algorithm are different from those obtained by the backward one. Nevertheless, the maximum number of identifiable error parameters obtained by both is the same, i.e. $N_{Serial} = 4n_r + 2n_p + 6$, including n encoder offsets and $N = 4n_r + 2n_p + 6 - n$ independent structural errors.

Adding subscripts 'ta' and 'ts' to identify the independent unit twists associated with the encoder offsets and the structural errors, and reordering them in sequence from the base to the end-link, finally results in the linearized minimal error model of serial kinematic chains.

$$\boldsymbol{\xi} = \boldsymbol{T}_a \boldsymbol{\eta}_a + \boldsymbol{T}_s \boldsymbol{\eta}_s \tag{5}$$

$$\boldsymbol{T}_a = \begin{bmatrix} \hat{\boldsymbol{\xi}}_{ta,1} & \cdots & \hat{\boldsymbol{\xi}}_{ta,n} \end{bmatrix} \in R^{6\times n}, \quad \boldsymbol{\eta}_a = \begin{pmatrix} \eta_{a,1} & \cdots & \eta_{a,n} \end{pmatrix}^{\mathrm{T}} \in R^{n}$$

$$\hat{\boldsymbol{\xi}}_{ta,j} = t\begin{pmatrix} \boldsymbol{w}_j \\ \boldsymbol{0} \end{pmatrix} + (1-t)\begin{pmatrix} \boldsymbol{r}_{j/n+2} \times \boldsymbol{w}_j \\ \boldsymbol{w}_j \end{pmatrix}, \quad \eta_{a,j} = t\delta d_j + (1-t)\delta\theta_j, \quad t = \begin{cases} 1 & \text{prismatic joint} \\ 0 & \text{revolute joint} \end{cases}$$

$$\boldsymbol{T}_s = \begin{bmatrix} \hat{\boldsymbol{\xi}}_{ts,1} & \ldots & \hat{\boldsymbol{\xi}}_{ts,N} \end{bmatrix} \in R^{6\times N}, \quad \boldsymbol{\eta}_s = \begin{pmatrix} \eta_{s,1} & \cdots & \eta_{s,N} \end{pmatrix}^{\mathrm{T}} \in R^{N}$$

where $\eta_{a,j}$ and $\hat{\boldsymbol{\xi}}_{ta,j}$ are the encoder offset of the jth actuated joint and its unit twist; $\eta_{s,j}$ and $\hat{\boldsymbol{\xi}}_{ts,j}$ are the jth structural error and its unit twist.

3. Minimal Error Model of Parallel Manipulators

3.1 Error modeling

Fig.4 shows the schematic diagram of an f-DOF ($2 \le f < 6$) parallel manipulator composed of l ($f \le l \le f+1$) limbs connecting the platform with the base. We assume that the ith limb contains n_i ($f \le n_i \le 6$, $i = 1, 2, \ldots, l$) 1-DOF joints, with at most one of them actuated. Without losing generality, two families of parallel manipulators are considered. The first family covers those with f constrained active limbs, i.e., $n_i < 6$ for all limbs. The second contains those having f unconstrained active limbs (i.e., $n_i = 6$, $i = 1, 2, \ldots, f$) plus one properly constrained passive limb numbered $l = f + 1$. Parallel manipulators not belonging to these families can be treated by methods similar to that used here.

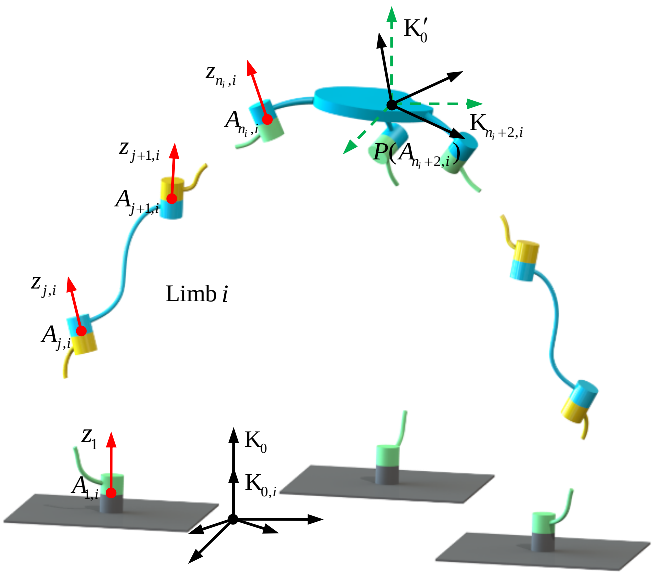

Fig. 4 The schematic diagram of a parallel manipulator

Using the conventions adopted in Section 2 for the error modeling of serial kinematic chains, a global reference frame K_0 is placed on the base and body frames $K_{j,i}$ ($j = 0, 1, \ldots, n_i + 2$) associated with the links of the ith limb. The moving reference frame K_0' has its origin at $P(A_{n_i+2,i})$ with its axes remaining parallel to those of K_0. Note that no errors of $K_{0,i}$ with respect to K_0 need be considered because those of $K_{1,i}$ with respect to $K_{0,i}$ have already been taken into account instead, and that all $K_{n_i+2,i}$ are coincident with one another because they can be arbitrarily located.

All the limbs share the same platform, so following the procedure to generate Eqs.(4) and (5) allows the pose error twist about $P(A_{n_i+2,i})$ to be expressed as

$$\boldsymbol{\xi} = \boldsymbol{\xi}_i = \boldsymbol{T}_{a,i} \boldsymbol{\eta}_{a,i} + \boldsymbol{T}_{s,i} \boldsymbol{\eta}_{s,i}, \quad i = 1, 2, \ldots, l \tag{6}$$

Then, using the method given in [44] to determine all the unit wrenches imposed by the ith limb upon the platform and collecting them in a matrix form, yields

$$\boldsymbol{W}_i = \begin{bmatrix} \boldsymbol{W}_{a,i} & \boldsymbol{W}_{c,i} \end{bmatrix}, \quad \boldsymbol{W}_{a,i} = \hat{\boldsymbol{\xi}}_{wa,g_i,i}, \quad \boldsymbol{W}_{c,i} = \begin{bmatrix} \hat{\boldsymbol{\xi}}_{wc,1,i} & \cdots & \hat{\boldsymbol{\xi}}_{wc,6-n_i,i} \end{bmatrix} \tag{7}$$

where $\hat{\boldsymbol{\xi}}_{wa,g_i,i}$ denotes the unit wrench of actuation generated by the actuated joint numbered g_i, and $\hat{\boldsymbol{\xi}}_{wc,k_c,i}$ the k_cth ($k_c = 1,2,\cdots,6-n_i$) unit wrench of constraint of the ith limb. Both are expressed in ray-coordinates. Obviously, $\boldsymbol{W}_{a,f+1} = \varnothing$ and $\boldsymbol{W}_{c,i} = \varnothing$ ($i = 1,2,\cdots,f$) for the second family of parallel manipulators.

Pre-multiplying on both sides of Eq.(6) with $\boldsymbol{W}_i^{\mathrm{T}}$ ($i = 1,2,\cdots,l$) and noting that a unit wrench of actuation (constraint) does virtual work only on a unit twist produced by that wrench [41–43], results in the linearized error model of parallel manipulators

$$\boldsymbol{W}^{\mathrm{T}}\boldsymbol{\xi} = \boldsymbol{\Lambda}_a\boldsymbol{\eta}_a + \boldsymbol{\Lambda}_s\boldsymbol{\eta}_s \tag{8}$$

$$\boldsymbol{W} = \begin{bmatrix} \boldsymbol{W}_1 & \cdots & \boldsymbol{W}_l \end{bmatrix}, \quad \boldsymbol{\Lambda}_a = \mathrm{diag}\begin{bmatrix} \boldsymbol{\Lambda}_{a,1} & \cdots & \boldsymbol{\Lambda}_{a,f} \end{bmatrix}, \quad \boldsymbol{\Lambda}_s = \mathrm{diag}\begin{bmatrix} \boldsymbol{\Lambda}_{s,1} & \cdots & \boldsymbol{\Lambda}_{s,l} \end{bmatrix}$$

$$\boldsymbol{\Lambda}_{a,k} = \begin{pmatrix} \hat{\boldsymbol{\xi}}_{wa,g_k,k}^{\mathrm{T}}\hat{\boldsymbol{\xi}}_{ta,g_k,k} \\ \boldsymbol{0}_{(6-n_k)\times 1} \end{pmatrix}, \quad \boldsymbol{\Lambda}_{s,i} = \boldsymbol{W}_i^{\mathrm{T}}\boldsymbol{T}_{s,i}, \quad \boldsymbol{T}_{s,i} = \begin{bmatrix} \hat{\boldsymbol{\xi}}_{ts,1,i} & \cdots & \hat{\boldsymbol{\xi}}_{ts,N_i,i} \end{bmatrix}$$

$$\boldsymbol{\eta}_a = \begin{pmatrix} \eta_{a,g_1,1} & \cdots & \eta_{a,g_f,f} \end{pmatrix}^{\mathrm{T}}, \quad \boldsymbol{\eta}_s = \begin{pmatrix} \boldsymbol{\eta}_{s,1}^{\mathrm{T}} & \cdots & \boldsymbol{\eta}_{s,l}^{\mathrm{T}} \end{pmatrix}^{\mathrm{T}}, \quad \boldsymbol{\eta}_{s,i} = \begin{pmatrix} \eta_{s,1,i} & \cdots & \eta_{s,N_i,i} \end{pmatrix}^{\mathrm{T}}$$

where $N_i = 4n_{r,i} + 2n_{p,i} + 6 - n_i$ denotes the number of structural errors within the ith limb. Adding the encoder offsets of the f actuated joints, then gives the total number of geometric error parameters of a parallel manipulator as

$$\bar{N}_{parallel} = f + \sum_{i=1}^{l} N_i \tag{9}$$

For non-overconstrained and non-redundantly actuated parallel manipulators, substituting the G-K mobility criterion $f = 6 - \sum_{i=1}^{l}(6-n_i)$ into Eq.(9) finally results in

$$\bar{N}_{parallel} = \sum_{i=1}^{l}\left(4n_{r,i} + 2n_{p,i}\right) + 6 = 4n_r + 2n_p + 6 \tag{10}$$

This formula is identical to that proposed by [40]. Note, however, that $\bar{N}_{parallel}$ given by Eq.(10) is not the number of identifiable error parameters of parallel manipulators, a claim to be justified in the following section.

3.2 Determination of the unidentifiable structural errors in a limb

All encoder offsets of parallel manipulators are identifiable if $\hat{\boldsymbol{\xi}}_{wa,g_k,k}^{\mathrm{T}}\hat{\boldsymbol{\xi}}_{ta,g_k,k} \neq 0$ ($k = 1,2,\cdots,f$) and $\boldsymbol{W}$ is non-singular. However, it is not generally true that all the structural errors given in Eq.(8) are identifiable. This limitation is proven by expanding $\boldsymbol{\Lambda}_{s,i}\boldsymbol{\eta}_{s,i}$ in Eq.(8) as

$$\boldsymbol{\Lambda}_{s,i}\boldsymbol{\eta}_{s,i} = \boldsymbol{W}_i^{\mathrm{T}}\boldsymbol{T}_{s,i}\boldsymbol{\eta}_{s,i} = \sum_{j=1}^{N_i}\eta_{s,j,i}\boldsymbol{W}_i^{\mathrm{T}}\hat{\boldsymbol{\xi}}_{ts,j,i}, \quad \boldsymbol{W}_i = \begin{bmatrix} \hat{\boldsymbol{\xi}}_{wa,g_i,i} & \hat{\boldsymbol{\xi}}_{wc,1,i} & \cdots & \hat{\boldsymbol{\xi}}_{wc,6-n_i,i} \end{bmatrix}, \quad i = 1,2,\cdots,l \tag{11}$$

Omitting, for convenience in this argument, the indicators "i" for limbs, "a" and "c" for actuations and constraints, and "s" for structural errors, Eq.(11) can be rewritten as

$$\boldsymbol{\Lambda}\boldsymbol{\eta} = \sum_{j=1}^{N}\eta_j\boldsymbol{W}^{\mathrm{T}}\hat{\boldsymbol{\xi}}_{t,j}, \quad \boldsymbol{W} = \begin{bmatrix} \hat{\boldsymbol{\xi}}_{w,1} & \cdots & \hat{\boldsymbol{\xi}}_{w,m} \end{bmatrix} \tag{12}$$

where m denotes the total number of the unit wrenches imposed by a limb on the platform. Obviously, if

$$\hat{\boldsymbol{\xi}}_{w,k}^{\mathrm{T}}\hat{\boldsymbol{\xi}}_{t,j} = 0 \quad \forall\hat{\boldsymbol{\xi}}_{w,k} \in \boldsymbol{W} \quad \text{or} \quad \hat{\boldsymbol{\xi}}_{t,j} \in \mathrm{Ker}\left(\boldsymbol{W}^{\mathrm{T}}\right) \tag{13}$$

then η_j is unidentifiable. Mathematically, Eq.(13) indicates that η_j is intrinsically unidentifiable if $\hat{\boldsymbol{\xi}}_{t,j}$ belongs to the null space of $\boldsymbol{W}^{\mathrm{T}}$, because it cannot be observed in the pose error measurements.

In the linearized model at a given configuration the Jacobian is generated using the nominal dimensional parameters. Therefore, the reciprocal relations of the wrenches/twists are ideal according to the Taylor's expansion. Note that $\hat{\xi}_{t,j}$ is always a screw in the form either a line vector or a free vector, and so is $\hat{\xi}_{w,k}$ for the limbs commonly used in parallel manipulators [44]. The geometric conditions satisfying Eq.(13) are revealed by considering two possible cases below; when both $\hat{\xi}_{w,k}$ and $\hat{\xi}_{t,j}$ are free vectors, Eq.(13) is self-satisfied.

Case 1: Both $\hat{\xi}_{w,k}$ and $\hat{\xi}_{t,j}$ are line vectors, physically representing a force and an instantaneous rotation, i.e.

$$\hat{\xi}_{w,k}=\begin{pmatrix}\boldsymbol{s}_{w,k}\\ \boldsymbol{r}_{w,k}\times\boldsymbol{s}_{w,k}\end{pmatrix},\quad \hat{\xi}_{t,j}=\begin{pmatrix}\boldsymbol{r}_{t,j}\times\boldsymbol{s}_{t,j}\\ \boldsymbol{s}_{t,j}\end{pmatrix}\tag{14}$$

where $\boldsymbol{s}_{w,k}$ ($\boldsymbol{s}_{t,j}$) denotes the unit vector of screw axis of $\hat{\xi}_{w,k}$ ($\hat{\xi}_{t,j}$), $\boldsymbol{r}_{w,k}$ ($\boldsymbol{r}_{t,j}$) denotes the position vector pointing from the origin of K_0' to an arbitrary point on the screw axis. Then

$$\hat{\xi}_{w,k}^{\mathrm{T}}\hat{\xi}_{t,j}=\left(\boldsymbol{r}_{w,k}-\boldsymbol{r}_{t,j}\right)^{\mathrm{T}}\left(\boldsymbol{s}_{w,k}\times\boldsymbol{s}_{t,j}\right)\equiv 0\tag{15}$$

if $\boldsymbol{s}_{w,k}$ and $\boldsymbol{s}_{t,j}$ are coplanar. One example satisfying Eq.(13) is that $\boldsymbol{s}_{w,k}$ intersects $\boldsymbol{s}_{t,j}$ because a pure force passing through the center of a spherical joint does no virtual work on the instantaneous rotation about an axis passing though the same center. Consequently, the angular structural error related to the instantaneous rotation is potentially unidentifiable.

Case 2: If $\hat{\xi}_{w,k}$ is a line vector while $\hat{\xi}_{t,j}$ is a free vector, or *vice versa*, i.e.

$$\hat{\xi}_{w,k}=\begin{pmatrix}\boldsymbol{s}_{w,k}\\ \boldsymbol{r}_{w,k}\times\boldsymbol{s}_{w,k}\end{pmatrix},\quad \hat{\xi}_{t,j}=\begin{pmatrix}\boldsymbol{s}_{t,j}\\ \boldsymbol{0}\end{pmatrix}\quad\text{or}\ \hat{\xi}_{w,k}=\begin{pmatrix}\boldsymbol{0}\\ \boldsymbol{s}_{w,k}\end{pmatrix},\quad \hat{\xi}_{t,j}=\begin{pmatrix}\boldsymbol{r}_{t,j}\times\boldsymbol{s}_{t,j}\\ \boldsymbol{s}_{t,j}\end{pmatrix}\tag{16}$$

then

$$\hat{\xi}_{w,k}^{\mathrm{T}}\hat{\xi}_{t,j}=\boldsymbol{s}_{w,k}^{\mathrm{T}}\boldsymbol{s}_{t,j}\equiv 0\tag{17}$$

requires $\boldsymbol{s}_{w,k}\perp\boldsymbol{s}_{t,j}$. This means that if the direction of a force (couple) is normal to that of an instantaneous translation (rotation), the linear (angular) structural error related to the instantaneous motion is potentially unidentifiable.

Fig.5 shows the flow chart of the algorithm for determining the unidentifiable parameters. The design freedom of a passive joint clearly offers no structural error, so, with $N_{p,i}$ the number of passive joints and $N_{0,i}$ the number unidentifiable structural errors of the ith limb detected by Eqs.(15) and (17), the total number of identifiable error parameters, including both encoder offsets and identifiable structural errors, of parallel manipulators is given by

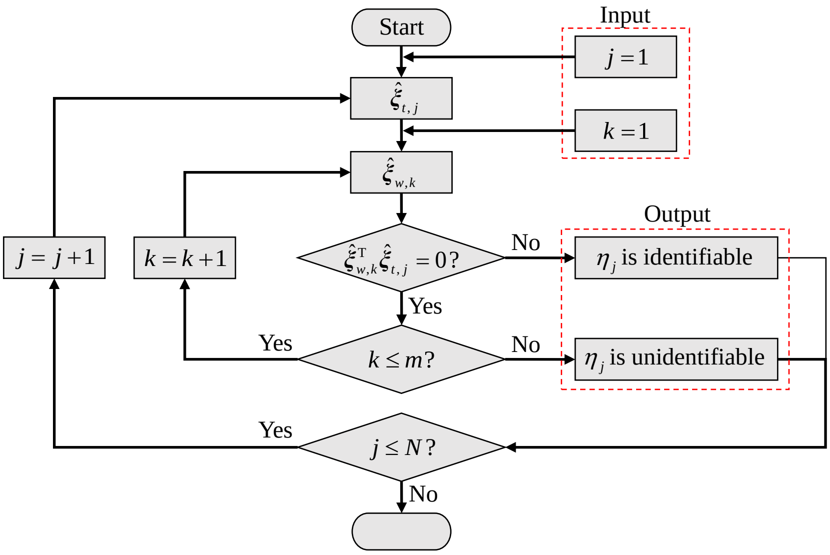

Fig. 5 The algorithm for determining the unidentifiable parameters

$$N_{parallel} = \sum_{i=1}^{l} \left(4n_{r,i} + 2n_{p,i} + 6 - N_{p,i} - N_{0,i} \right) \tag{18}$$

At this stage, it is important to note that the identifiability of a structural error within the error model given in Eq. (8) is highly related to limb connectivity, to joint geometry and to the actuator arrangement of the parallel manipulator being considered. So, removing all unidentifiable structural errors from Eq.(8) finally results in the minimal linearized error model of parallel manipulators.

4. Examples

In this section, we take 3-R$\underline{\text{P}}$S and 3-U$\underline{\text{P}}$S&UP parallel mechanisms as two exemplars to illustrate the effectiveness of the proposed process for determining redundant error parameters within limbs using the method developed in Section 2, and for detecting unidentifiable structural errors of the parallel mechanisms using the criteria developed in Section 3. Here, S, U, P, R denote spherical, universal, prismatic and revolute joints, respectively. The underlined $\underline{\text{P}}$ denotes the actuated prismatic joint. For modelling, the S and U joints are replaced by the appropriate number of revolute joints, denoted by R, having mutually orthogonal axes.

4.1. 3-RPS parallel mechanism

Fig.6(a) shows schematic diagram of a 3-R$\underline{\text{P}}$S parallel mechanism compromising a base, a platform and three identical R$\underline{\text{P}}$S limbs. By omitting indicator '*i*' for limbs, Fig.6(b) shows a R$\underline{\text{P}}$S limb whose joint axes are arranged to satisfy the geometric conditions below

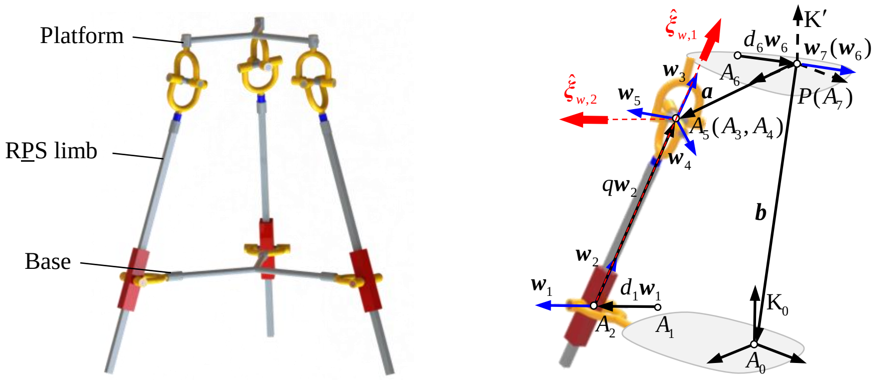

(a) 3-R$\underline{\text{P}}$S parallel mechanism (b) a R$\underline{\text{P}}$S limb

Fig. 6 The schematic diagram of a 3-R$\underline{\text{P}}$S parallel mechanism

$$\boldsymbol{w}_1 \perp \boldsymbol{w}_2,\ \boldsymbol{w}_2 = \boldsymbol{w}_3,\ \boldsymbol{w}_3 \perp \boldsymbol{w}_4,\ \boldsymbol{w}_4 \perp \boldsymbol{w}_5 \tag{19}$$

Keeping mind $n = 5$, $n_r = 4$ and $n_p = 1$, and removing all the redundant error terms while retaining the encoder offset of the $\underline{\text{P}}$ joint using the method developed in Section 2, leads to

$$N = 4n_r + 2n_p + 6 - n = 4\times4 + 2\times1 + 6 - 5 = 19 \tag{20}$$

non-redundant structural errors given in Table 1. The unit twists associated with these error terms are given by

$$\hat{\xi}_{t,1} = \begin{pmatrix} \boldsymbol{b}\times\boldsymbol{w}_0 \\ \boldsymbol{w}_0 \end{pmatrix},\ \hat{\xi}_{t,2} = \begin{pmatrix} \boldsymbol{w}_0 \\ \boldsymbol{0} \end{pmatrix},\ \hat{\xi}_{t,3} = \begin{pmatrix} \boldsymbol{u}_1 \\ \boldsymbol{0} \end{pmatrix},\ \hat{\xi}_{t,4} = \begin{pmatrix} (\boldsymbol{a} - q\boldsymbol{w}_2 - d_1\boldsymbol{w}_1)\times\boldsymbol{u}_1 \\ \boldsymbol{u}_1 \end{pmatrix}$$

$$\hat{\xi}_{t,5} = \begin{pmatrix} \boldsymbol{w}_1 \\ \boldsymbol{0} \end{pmatrix},\ \hat{\xi}_{t,6} = \begin{pmatrix} (\boldsymbol{a} - q\boldsymbol{w}_2)\times\boldsymbol{u}_2 \\ \boldsymbol{u}_2 \end{pmatrix}$$

$$\hat{\xi}_{t,7} = \begin{pmatrix} \boldsymbol{a}\times\boldsymbol{w}_2 \\ \boldsymbol{w}_2 \end{pmatrix},\ \hat{\xi}_{t,8} = \begin{pmatrix} \boldsymbol{a}\times\boldsymbol{u}_3 \\ \boldsymbol{u}_3 \end{pmatrix},\ \hat{\xi}_{t,9} = \begin{pmatrix} \boldsymbol{a}\times\boldsymbol{v}_3 \\ \boldsymbol{v}_3 \end{pmatrix}$$

$$\hat{\xi}_{t,10} = \begin{pmatrix} \boldsymbol{u}_4 \\ \boldsymbol{0} \end{pmatrix},\ \hat{\xi}_{t,11} = \begin{pmatrix} \boldsymbol{a}\times\boldsymbol{u}_4 \\ \boldsymbol{u}_4 \end{pmatrix}$$

$$\hat{\xi}_{t,12}=\begin{pmatrix}\boldsymbol{w}_4\\ \boldsymbol{0}\end{pmatrix},\ \hat{\xi}_{t,13}=\begin{pmatrix}\boldsymbol{u}_5\\ \boldsymbol{0}\end{pmatrix},\ \hat{\xi}_{t,14}=\begin{pmatrix}\boldsymbol{a}\times\boldsymbol{u}_5\\ \boldsymbol{u}_5\end{pmatrix}$$
$$\hat{\xi}_{t,15}=\begin{pmatrix}\boldsymbol{w}_5\\ \boldsymbol{0}\end{pmatrix},\ \hat{\xi}_{t,16}=\begin{pmatrix}\boldsymbol{u}_6\\ \boldsymbol{0}\end{pmatrix},\ \hat{\xi}_{t,17}=\begin{pmatrix}-d_6\boldsymbol{w}_6\times\boldsymbol{u}_6\\ \boldsymbol{u}_6\end{pmatrix}$$
$$\hat{\xi}_{t,18}=\begin{pmatrix}\boldsymbol{0}\\ \boldsymbol{w}_6\end{pmatrix},\ \hat{\xi}_{t,19}=\begin{pmatrix}\boldsymbol{w}_6\\ \boldsymbol{0}\end{pmatrix} \tag{21}$$

where d_j ($j=1,6$) denotes the common normal between the x_j and x_{j+1} axes, $q=\left\|\overrightarrow{A_2A_5}\right\|$, $\boldsymbol{a}=\left\|\overrightarrow{PA_5}\right\|$ and $\boldsymbol{b}=\left\|\overrightarrow{PA_0}\right\|$, respectively. The RPS limb imposes on the platform a unit wrench of actuation and a unit wrench of constraint, both are in the form of line vectors as depicted in Fig.6(b).

$$\hat{\xi}_{w,1}=\hat{\xi}_{wa,2}=\begin{pmatrix}\boldsymbol{w}_2\\ \boldsymbol{a}\times\boldsymbol{w}_2\end{pmatrix},\quad \hat{\xi}_{w,2}=\hat{\xi}_{wc,1}=\begin{pmatrix}\boldsymbol{w}_1\\ \boldsymbol{a}\times\boldsymbol{w}_1\end{pmatrix} \tag{22}$$

Examination of Eq.(21) and (22) shows that $\hat{\xi}_{t,j}\,(j=7,\ 8,\ 9,\ 11,\ 14)$ are line vectors having their screw axes intersecting the screw axis of $\hat{\xi}_{w,1}$ and $\hat{\xi}_{w,2}$. Consequently, there are 5 unidentifiable structural errors (shown in red in Table 1) that can be detected using the criteria developed in Eq.(15).

With $l=3$, $N_{p,i}=4$ and $N_{0,i}=5$ ($i=1,2,3$), the number of identifiable error parameters of the 3-RPS parallel manipulator can be determined by

$$N_{\text{3-RPS}}=\sum_{i=1}^{3}\left(4n_{r,i}+2n_{p,i}+6-N_{p,i}-N_{0,i}\right)=\sum_{i=1}^{3}\left(4\times4+2\times1+6-4-5\right)=45 \tag{23}$$

It contains 3 encoder offsets of the actuated prismatic joints and 42 identifiable structural errors in total.

4.2. 3-UPS&UP parallel mechanism

Fig.7(a) shows schematic diagram of a 3-UPS&UP parallel mechanism composed of a base, a platform, three identical UPS limbs plus a UP limb in the middle, where the UP limb connects rigidly to the platform. Figs.7(b) and (c) show joint axe arrangements of these limbs, which satisfy the geometric conditions

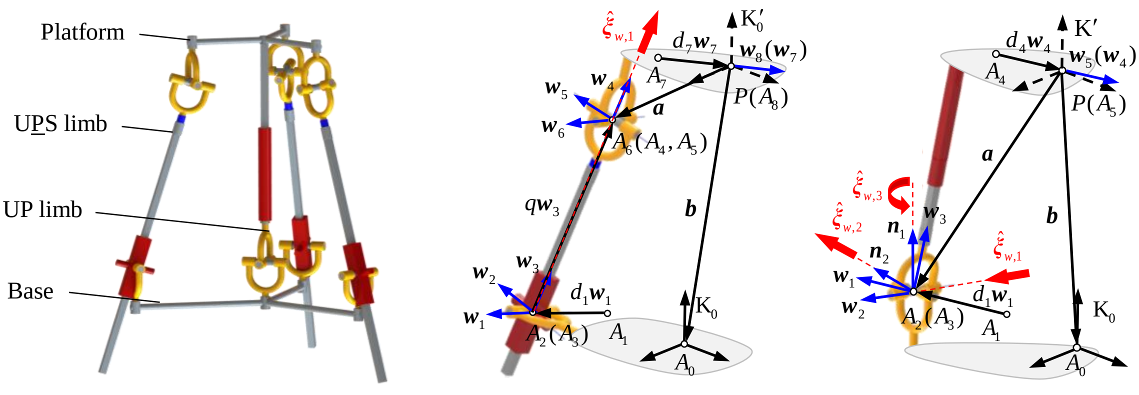

(a) 3-UPS&UP parallel mechanism (b) a UPS limb (c) a UP limb

Fig. 7 The schematic diagram of a 3-UPS&UP parallel mechanism

UPS limb:

$$\boldsymbol{w}_1\perp\boldsymbol{w}_2,\ \boldsymbol{w}_2\perp\boldsymbol{w}_3,\ \boldsymbol{w}_2=\boldsymbol{w}_3,\ \boldsymbol{w}_4\perp\boldsymbol{w}_5,\ \boldsymbol{w}_5\perp\boldsymbol{w}_6 \tag{24}$$

UP limb:

$$\boldsymbol{w}_1\perp\boldsymbol{w}_2,\ \boldsymbol{w}_2\perp\boldsymbol{w}_3,\ \boldsymbol{n}_1=\boldsymbol{w}_1\times\boldsymbol{w}_2,\ \boldsymbol{n}_2=\boldsymbol{w}_2\times\boldsymbol{w}_3 \tag{25}$$

Clearly, the number of non-redundant structural errors in the U$\underline{\text{P}}$S limb is $N=22$ as $n=5$, $n_r=4$ and $n_p=1$, and that for the UP limb is $N=13$ as $n=3$, $n_r=2$ and $n_p=1$. The corresponding error terms are given in Tables 1.

On one hand, the unit twists associated with the non-redundant structural errors in the U$\underline{\text{P}}$S limb can be formulated as

$$\begin{gathered}
\hat{\xi}_{t,1}=\begin{pmatrix}\boldsymbol{b}\times\boldsymbol{w}_0\\ \boldsymbol{w}_0\end{pmatrix},\ \hat{\xi}_{t,2}=\begin{pmatrix}\boldsymbol{w}_0\\ \boldsymbol{0}\end{pmatrix},\ \hat{\xi}_{t,3}=\begin{pmatrix}\boldsymbol{u}_1\\ \boldsymbol{0}\end{pmatrix},\ \hat{\xi}_{t,4}=\begin{pmatrix}(\boldsymbol{a}-q\boldsymbol{w}_3-d_1\boldsymbol{w}_1)\times\boldsymbol{u}_1\\ \boldsymbol{u}_1\end{pmatrix}\\
\hat{\xi}_{t,5}=\begin{pmatrix}\boldsymbol{w}_1\\ \boldsymbol{0}\end{pmatrix},\ \hat{\xi}_{t,6}=\begin{pmatrix}\boldsymbol{u}_2\\ \boldsymbol{0}\end{pmatrix},\ \hat{\xi}_{t,7}=\begin{pmatrix}(\boldsymbol{a}-q\boldsymbol{w}_3)\times\boldsymbol{u}_2\\ \boldsymbol{u}_2\end{pmatrix}\\
\hat{\xi}_{t,8}=\begin{pmatrix}\boldsymbol{w}_2\\ \boldsymbol{0}\end{pmatrix},\ \hat{\xi}_{t,9}=\begin{pmatrix}(\boldsymbol{a}-q\boldsymbol{w}_3)\times\boldsymbol{u}_3\\ \boldsymbol{u}_3\end{pmatrix}\\
\hat{\xi}_{t,10}=\begin{pmatrix}\boldsymbol{a}\times\boldsymbol{w}_3\\ \boldsymbol{w}_3\end{pmatrix},\ \hat{\xi}_{t,11}=\begin{pmatrix}\boldsymbol{a}\times\boldsymbol{u}_4\\ \boldsymbol{u}_4\end{pmatrix},\ \hat{\xi}_{t,12}=\begin{pmatrix}\boldsymbol{a}\times\boldsymbol{v}_4\\ \boldsymbol{v}_4\end{pmatrix}\\
\hat{\xi}_{t,13}=\begin{pmatrix}\boldsymbol{u}_5\\ \boldsymbol{0}\end{pmatrix},\ \hat{\xi}_{t,14}=\begin{pmatrix}\boldsymbol{a}\times\boldsymbol{u}_5\\ \boldsymbol{u}_5\end{pmatrix}\\
\hat{\xi}_{t,15}=\begin{pmatrix}\boldsymbol{w}_5\\ \boldsymbol{0}\end{pmatrix},\ \hat{\xi}_{t,16}=\begin{pmatrix}\boldsymbol{u}_6\\ \boldsymbol{0}\end{pmatrix},\ \hat{\xi}_{t,17}=\begin{pmatrix}\boldsymbol{a}\times\boldsymbol{u}_6\\ \boldsymbol{u}_6\end{pmatrix}\\
\hat{\xi}_{t,18}=\begin{pmatrix}\boldsymbol{w}_6\\ \boldsymbol{0}\end{pmatrix},\ \hat{\xi}_{t,19}=\begin{pmatrix}\boldsymbol{u}_7\\ \boldsymbol{0}\end{pmatrix},\ \hat{\xi}_{t,20}=\begin{pmatrix}-d_7\boldsymbol{w}_7\times\boldsymbol{u}_7\\ \boldsymbol{u}_7\end{pmatrix}\\
\hat{\xi}_{t,21}=\begin{pmatrix}\boldsymbol{0}\\ \boldsymbol{w}_7\end{pmatrix},\ \hat{\xi}_{t,22}=\begin{pmatrix}\boldsymbol{w}_7\\ \boldsymbol{0}\end{pmatrix}
\end{gathered}\tag{26}$$

Note that the limb imposes on the platform a unit wrench of actuation in the form of line vector as shown in Fig.7(b).

$$\hat{\xi}_{wa,3}=\hat{\xi}_{w,1}=\begin{pmatrix}\boldsymbol{w}_3\\ \boldsymbol{a}\times\boldsymbol{w}_3\end{pmatrix}\tag{27}$$

It can be seen from Eq.(26) and (27) that $\hat{\xi}_{t,j}\,(j=7,\ 9\sim12,\ 14,\ 17)$ are line vectors having their screw axes intersecting the screw axis of $\hat{\xi}_{w,1}$; while $\hat{\xi}_{t,j}\,(j=8,\ 13,\ 15)$ are free vectors having their screw axes normal to the screw axis of $\hat{\xi}_{w,1}$. Consequently, there are 10 unidentifiable structural errors (shown in red in Table 1) that can be detected using the criteria given in Eqs.(15) and (17).

On the other hand, the unit twists associated with the non-redundant structural errors in the UP limb can be formulated by

$$\begin{gathered}
\hat{\xi}_{t,1}=\begin{pmatrix}\boldsymbol{b}\times\boldsymbol{w}_0\\ \boldsymbol{w}_0\end{pmatrix},\ \hat{\xi}_{t,2}=\begin{pmatrix}\boldsymbol{w}_0\\ \boldsymbol{0}\end{pmatrix},\ \hat{\xi}_{t,3}=\begin{pmatrix}\boldsymbol{u}_1\\ \boldsymbol{0}\end{pmatrix},\ \hat{\xi}_{t,4}=\begin{pmatrix}(\boldsymbol{a}-d_1\boldsymbol{w}_1)\times\boldsymbol{u}_1\\ \boldsymbol{u}_1\end{pmatrix}\\
\hat{\xi}_{t,5}=\begin{pmatrix}\boldsymbol{w}_1\\ \boldsymbol{0}\end{pmatrix},\ \hat{\xi}_{t,6}=\begin{pmatrix}\boldsymbol{u}_2\\ \boldsymbol{0}\end{pmatrix},\ \hat{\xi}_{t,7}=\begin{pmatrix}\boldsymbol{a}\times\boldsymbol{u}_2\\ \boldsymbol{u}_2\end{pmatrix}\\
\hat{\xi}_{t,8}=\begin{pmatrix}\boldsymbol{w}_2\\ \boldsymbol{0}\end{pmatrix},\ \hat{\xi}_{t,9}=\begin{pmatrix}\boldsymbol{a}\times\boldsymbol{u}_3\\ \boldsymbol{u}_3\end{pmatrix}\\
\hat{\xi}_{t,10}=\begin{pmatrix}\boldsymbol{a}\times\boldsymbol{w}_3\\ \boldsymbol{w}_3\end{pmatrix},\ \hat{\xi}_{t,11}=\begin{pmatrix}-d_4\boldsymbol{w}_4\times\boldsymbol{u}_4\\ \boldsymbol{u}_4\end{pmatrix}\\
\hat{\xi}_{t,12}=\begin{pmatrix}\boldsymbol{0}\\ \boldsymbol{w}_4\end{pmatrix},\ \hat{\xi}_{t,13}=\begin{pmatrix}\boldsymbol{w}_4\\ \boldsymbol{0}\end{pmatrix}
\end{gathered}\tag{28}$$

The limb imposes on the platform three unit wrenches of constraint, i.e. two linear vectors and one couple, as clearly depicted in Fig.7(c).

$$\hat{\xi}_{w,1} = \hat{\xi}_{wc,1} = \begin{pmatrix} \boldsymbol{w}_2 \\ \boldsymbol{a} \times \boldsymbol{w}_2 \end{pmatrix}, \quad \hat{\xi}_{w,2} = \hat{\xi}_{wc,2} = \begin{pmatrix} \boldsymbol{n}_2 \\ \boldsymbol{a} \times \boldsymbol{n}_2 \end{pmatrix}, \quad \hat{\xi}_{w,3} = \hat{\xi}_{wc,3} = \begin{pmatrix} \boldsymbol{0} \\ \boldsymbol{n}_1 \end{pmatrix} \tag{29}$$

It is easy to see from Eqs.(28) and (29) that the structural errors listed in Table 1 are identifiable since neither Eq.(15) nor Eq.(17) is satisfied.

With $N_{p,i} = 5$, $N_{0,i} = 10$ for $i = 1,2,3$ and $N_{p,i} = 3$, $N_{0,i} = 0$ for $i = 4$, the number of identifiable error parameters of the 3-UPS&UP parallel mechanism can then be determined by

$$\begin{aligned} N_{\text{3-UPS\&UP}} &= \sum_{i=1}^{4} \left(4n_{r,i} + 2n_{p,i} + 6 - N_{p,i} - N_{0,i} \right) \\ &= \sum_{i=1}^{3} \left(4\times5 + 2\times1 + 6 - 5 - 10 \right) + \left(4\times2 + 2\times1 + 6 - 3 - 0 \right) = 52 \end{aligned} \tag{30}$$

It contains 3 encoder offsets of the actuated prismatic joints and 49 identifiable structural errors in total.

The results given in Eq.(23) and Eq.(30) have been verified using the SVD method [27]. For parallel manipulators of other types, the number of identifiable geometric errors can also be determined straightforwardly according to Eq.(18), which include both encoder offsets and identifiable structural errors. For convenience, Table 1 summarizes the structural errors of several limb designs that contain one actuated/passive prismatic joint and are commonly used to build parallel kinematic machines. Also, the encoder offset of an actuated limb is indicated in the table. The wrenches of actuation and constraint imposed by each limb on the platform are determined using the method proposed in [44]. The non-redundant structural errors of each limb are determined using the method developed in Section 2, out of which the unidentifiable ones (shown in red) are detected using the criteria developed in Section 3.

Table 1 Encoder offset and structural errors in the limbs containing one prismatic joint

Limb types	Wrench of actuations	Wrench of constraints	Encoder offset	Structural errors
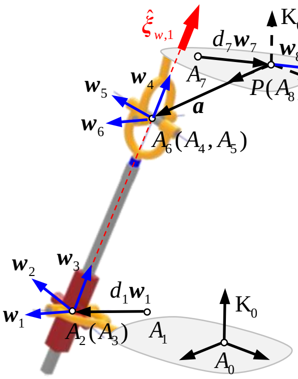 UPS	$\hat{\xi}_{wa,3} = \hat{\xi}_{w,1} = \begin{pmatrix} \boldsymbol{w}_3 \\ \boldsymbol{a}\times\boldsymbol{w}_3 \end{pmatrix}$	N/A	δd_3	$\delta\theta_0$, δd_0, δa_0, $\delta\alpha_0$, δd_1, δa_1, $\delta\alpha_1$, δd_2, $\delta\alpha_2$, $\delta\theta_3$, $\delta\alpha_3$, $\delta\beta_3$, δa_4, $\delta\alpha_4$, δd_5, δa_5, $\delta\alpha_5$, δd_6, δa_6, $\delta\alpha_6$, $\delta\theta_7$, δd_7
$\boldsymbol{w}_1 \perp \boldsymbol{w}_2$, $\boldsymbol{w}_2 \perp \boldsymbol{w}_3$, $\boldsymbol{w}_3 = \boldsymbol{w}_4$, $\boldsymbol{w}_4 \perp \boldsymbol{w}_5$, $\boldsymbol{w}_5 \perp \boldsymbol{w}_6$				
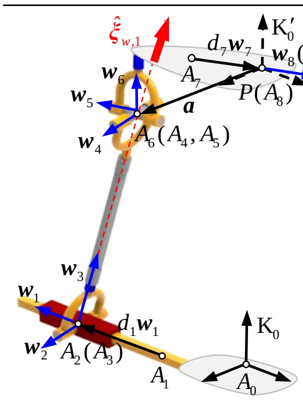 PUS	$\hat{\xi}_{wa,1} = \hat{\xi}_{w,1} = \begin{pmatrix} \boldsymbol{w}_3 \\ \boldsymbol{a}\times\boldsymbol{w}_3 \end{pmatrix}$	N/A	δd_1	$\delta\theta_0$, δd_0, $\delta\alpha_0$, $\delta\theta_1$, $\delta\alpha_1$, δd_2, δa_2, $\delta\alpha_2$, δd_3, δa_3, $\delta\alpha_3$, δd_4, δa_4, $\delta\alpha_4$, δd_5, δa_5, $\delta\alpha_5$, δd_6, δa_6, $\delta\alpha_6$, $\delta\theta_7$, δd_7
$\boldsymbol{w}_1 \perp \boldsymbol{w}_2$, $\boldsymbol{w}_2 \perp \boldsymbol{w}_3$, $\boldsymbol{w}_3 \perp \boldsymbol{w}_4$, $\boldsymbol{w}_4 \perp \boldsymbol{w}_5$, $\boldsymbol{w}_5 \perp \boldsymbol{w}_6$				

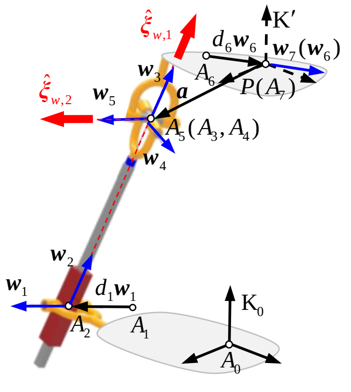 RPS	$\hat{\xi}_{wa,2}=\hat{\xi}_{w,1}=\begin{pmatrix}\boldsymbol{w}_2\\ \boldsymbol{a}\times\boldsymbol{w}_2\end{pmatrix}$ $\hat{\xi}_{wc,1}=\hat{\xi}_{w,2}=\begin{pmatrix}\boldsymbol{w}_1\\ \boldsymbol{a}\times\boldsymbol{w}_1\end{pmatrix}$	δd_2	$\delta\theta_0,\ \delta d_0,\ \delta a_0,\ \delta\alpha_0,$ $\delta d_1,\ \delta\alpha_1,$ $\delta\theta_2,\ \delta\alpha_2,\ \delta\beta_2,$ $\delta a_3,\ \delta\alpha_3,$ $\delta d_4,\ \delta a_4,\ \delta\alpha_4,$ $\delta d_5,\ \delta a_5,\ \delta\alpha_5,$ $\delta\theta_6,\ \delta d_6$
$\boldsymbol{w}_1\perp\boldsymbol{w}_2,\ \boldsymbol{w}_2=\boldsymbol{w}_3,\ \boldsymbol{w}_3\perp\boldsymbol{w}_4,\ \boldsymbol{w}_4\perp\boldsymbol{w}_5$			
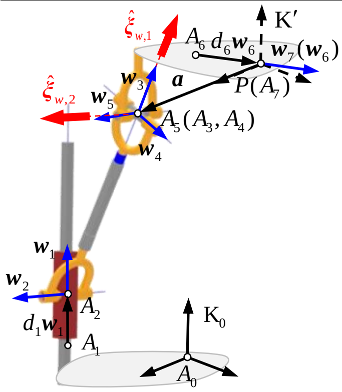 PRS	$\hat{\xi}_{wa,1}=\hat{\xi}_{w,1}=\begin{pmatrix}\boldsymbol{w}_3\\ \boldsymbol{a}\times\boldsymbol{w}_3\end{pmatrix}$ $\hat{\xi}_{wc,1}=\hat{\xi}_{w,2}=\begin{pmatrix}\boldsymbol{w}_2\\ \boldsymbol{a}\times\boldsymbol{w}_2\end{pmatrix}$	δd_1	$\delta\theta_0,\ \delta d_0,\ \delta\alpha_0,$ $\delta\theta_1,\ \delta\alpha_1,$ $\delta d_2,\ \delta a_2,\ \delta\alpha_2,$ $\delta d_3,\ \delta a_3,\ \delta\alpha_3,$ $\delta d_4,\ \delta a_4,\ \delta\alpha_4,$ $\delta d_5,\ \delta a_5,\ \delta\alpha_5,$ $\delta\theta_6,\ \delta d_6$
$\boldsymbol{w}_1\perp\boldsymbol{w}_2,\ \boldsymbol{w}_2\perp\boldsymbol{w}_3,\ \boldsymbol{w}_3\perp\boldsymbol{w}_4,\ \boldsymbol{w}_4\perp\boldsymbol{w}_5$			
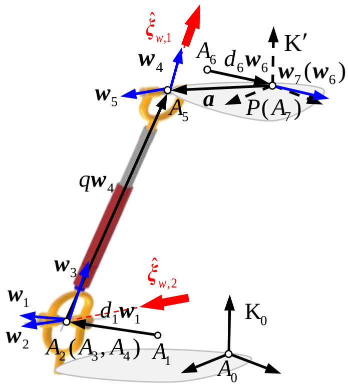 SPR	$\hat{\xi}_{wa,4}=\hat{\xi}_{w,1}=\begin{pmatrix}\boldsymbol{w}_4\\ \boldsymbol{a}\times\boldsymbol{w}_4\end{pmatrix}$ $\hat{\xi}_{wc,1}=\hat{\xi}_{w,2}=\begin{pmatrix}\boldsymbol{w}_5\\ (\boldsymbol{a}-q\boldsymbol{w}_4)\times\boldsymbol{w}_5\end{pmatrix}$	δd_4	$\delta\theta_0,\ \delta d_0,\ \delta a_0,\ \delta\alpha_0,$ $\delta d_1,\ \delta a_1,\ \delta\alpha_1,$ $\delta d_2,\ \delta a_2,\ \delta\alpha_2,$ $\delta\alpha_3,\ \delta\beta_3,$ $\delta\theta_4,\ \delta\alpha_4,$ $\delta d_5,\ \delta a_5,\ \delta\alpha_5,$ $\delta\theta_6,\ \delta d_6$
$\boldsymbol{w}_1\perp\boldsymbol{w}_2,\ \boldsymbol{w}_2\perp\boldsymbol{w}_3,\ \boldsymbol{w}_3=\boldsymbol{w}_4,\ \boldsymbol{w}_4\perp\boldsymbol{w}_5$			
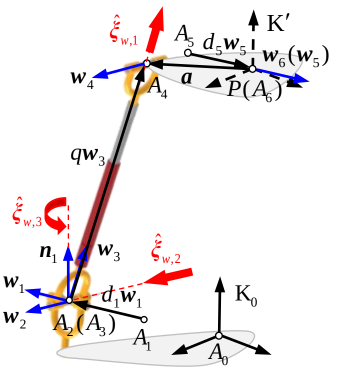 UPR	$\hat{\xi}_{wa,3}=\hat{\xi}_{w,1}=\begin{pmatrix}\boldsymbol{w}_3\\ \boldsymbol{a}\times\boldsymbol{w}_3\end{pmatrix}$ $\hat{\xi}_{wc,1}=\hat{\xi}_{w,2}=\begin{pmatrix}\boldsymbol{w}_2\\ (\boldsymbol{a}-q\boldsymbol{w}_3)\times\boldsymbol{w}_2\end{pmatrix}$ $\hat{\xi}_{wc,2}=\hat{\xi}_{w,3}=\begin{pmatrix}\boldsymbol{0}\\ \boldsymbol{n}_1\end{pmatrix}$ $\boldsymbol{n}_1=\boldsymbol{w}_1\times\boldsymbol{w}_2$	δd_3	$\delta\theta_0,\ \delta d_0,\ \delta a_0,\ \delta\alpha_0,$ $\delta d_1,\ \delta a_1,\ \delta\alpha_1,$ $\delta d_2,\ \delta\alpha_2,$ $\delta\theta_3,\ \delta\alpha_3,$ $\delta d_4,\ \delta a_4,\ \delta\alpha_4,$ $\delta\theta_5,\ \delta d_5$
$\boldsymbol{w}_1\perp\boldsymbol{w}_2,\ \boldsymbol{w}_2\perp\boldsymbol{w}_3,\ \boldsymbol{w}_3\perp\boldsymbol{w}_4,\ \boldsymbol{w}_4=\boldsymbol{w}_2$			

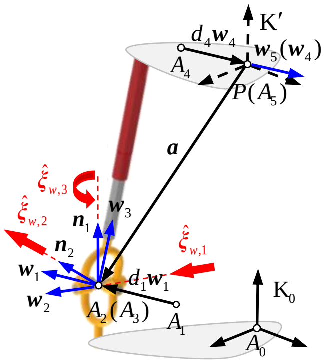	N/A	$\hat{\xi}_{wc,1}=\hat{\xi}_{w,1}=\begin{pmatrix}\boldsymbol{w}_2\\ \boldsymbol{a}\times\boldsymbol{w}_2\end{pmatrix}$ $\hat{\xi}_{wc,2}=\hat{\xi}_{w,2}=\begin{pmatrix}\boldsymbol{n}_2\\ \boldsymbol{a}\times\boldsymbol{n}_2\end{pmatrix}$ $\hat{\xi}_{wc,3}=\hat{\xi}_{w,3}=\begin{pmatrix}\boldsymbol{0}\\ \boldsymbol{n}_1\end{pmatrix}$ $\boldsymbol{n}_1=\boldsymbol{w}_1\times\boldsymbol{w}_2$, $\boldsymbol{n}_2=\boldsymbol{w}_2\times\boldsymbol{w}_3$	N/A	$\delta\theta_0$, δd_0, δa_0, $\delta\alpha_0$, δd_1, δa_1, $\delta\alpha_1$, δd_2, $\delta\alpha_2$, $\delta\theta_3$, $\delta\alpha_3$, $\delta\theta_4$, δd_4
UP				
$\boldsymbol{w}_1\perp\boldsymbol{w}_2$, $\boldsymbol{w}_2\perp\boldsymbol{w}_3$				

Note: The unidentifiable structural errors are marked in red

5. Conclusions

This paper presents a screw theory based approach to determining the identifiable error parameters of parallel manipulators for calibration purpose. The following conclusions are drawn.

(1) By using the modified D-H convention and considering the linear correlation analysis of a set of unit twists corresponding to the relevant axes of three consecutive body-fixed frames, we have proposed an approach that enables all encoder offsets to be retained in the minimal error model of serial kinematic chains.

(2) By examining the virtual work that the unit wrenches imposed by a limb delivery on the unit twist associated with a structural error belonging to that limb, we have created a vigorous criterion that allows the unidentifiable structural errors of parallel manipulators to be fully detected. This leads to a new formula for the determination of the maximum number of identifiable geometric errors, including both encoder offsets and identifiable structural errors, of parallel manipulators. We have shown that identifiability of a structural error is highly dependent upon the limb connectivity, joint geometry and actuator arrangement. Two examples have provided to show the procedure for determining the identifiable parameters of parallel mechanisms and the results have been consolidated by SVD method.

(3) The linearized error model established using the proposed method fulfills the requirements of completeness, continuity and minimality, thus enabling the efficient practical implementation of coarse plus fine calibration strategies for parallel manipulators.

Acknowledgement

This work is partially supported by National Natural Science Foundation of China (grants 51420105007, 51605324, and 51622508) and EU H2020-RISE-ECSASDP (grant 734272).

References

[1] P. Schellekens, N. Rosielle, H. Vermeulen, M. Vermeulen, S. Wetzels, W. Pril, Design for precision: current status and trends, CIRP Ann. - Manuf. Technol. 47(2) (1998) 557–586.

[2] B.W. Mooring, Z.S. Roth, M.R. Driels, Fundamentals of manipulator calibration, John Wiley & Sons, New York, NY, USA, (1991).

[3] B. Siciliano, O. Khatib, Springer handbook of robotics, 2nd ed., Springer, Berlin, Germany, (2016).

[4] J.P. Merlet, Parallel robots: open problems, in: J.M. Hollerbach, D.E. Koditschek (Eds.), Robotics Research, Springer, London, UK, (2000) 27–32.

[5] J. Denavit, R.S. Hartenberg, A kinematic notation for lower-pair mechanisms based on matrices, J. Appl. Mech. 22(2) (1955) 215–221.

[6] L.W. Tsai, Robot analysis: the mechanics of serial and parallel manipulators, John Wiley & Sons, New York, NY, USA, (1999).

[7] W. Veitschegger, C.H. Wu, Robot accuracy analysis based on kinematics, IEEE J. Robot. Autom. 2(3) (1986) 171–179.

[8] H.W. Stone, Kinematic modeling, identification, and control of robotic manipulators, Kluwer, Dordrecht, The Netherlands, (1987).

[9] S. Hayati, K. Tso, G. Roston, Robot geometry calibration, in: Proc. 1988 IEEE Int. Conf. Robot. Autom., Philadelphia, PA, USA, (1988) 947–951.

[10] H. Zhuang, Z.S. Roth, Robot calibration using the CPC error model, Robot. Comput. -Integr. Manuf. 9(3) (1992) 227–237.

[11] L.J. Everett, M.R. Driels, B.W. Mooring, Kinematic modelling for robot calibration, in: Proc. 1987 IEEE Int. Conf. Robot. Autom., Raleigh, NC, USA, (1987) 183–189.

[12] K. Schröer, S.L. Albright, M. Grethlein, Complete, minimal and model-continuous kinematic models for robot calibration, Robot. Comput. -Integr. Manuf. 13(1) (1997) 73–85.

[13] W. Zhu, B. Mei, Y. Ke, Kinematic modeling and parameter identification of a new circumferential drilling machine for aircraft assembly, Int. J. Adv. Manuf. Technol. 72(5) (2014) 1143–1158.

[14] Y. Wu, A. Klimchik, S. Caro, B. Furet, A. Pashkevich, Geometric calibration of industrial robots using enhanced partial pose measurements and design of experiments, Robot. Comput. -Integr. Manuf. 35 (2015) 151–168.

[15] F.C. Park, K. Okamura, Kinematic calibration and the product of exponentials formula, in: J. Lenarčič, B. Ravani (Eds.),

Advances in Robot Kinematics and Computational Geometry, Springer, Dordrecht, The Netherlands, (1994) 119–128.
[16] K. Okamura, F.C. Park, Kinematic calibration using the product of exponentials formula, Robotica 14(4) (1996) 415–421.
[17] I. Chen, G. Yang, C.T. Tan, H.Y. Song, Local POE model for robot kinematic calibration, Mech. Mach. Theory 36(11) (2001) 1215–1239.
[18] H. Wang, S. Shen, X. Lu, A screw axis identification method for serial robot calibration based on the POE model, Ind. Robot: Int. J. Rob. Res. Appl. 39 (2012) 146–153.
[19] C.C. Iurașcu, F.C. Park, Geometric algorithms for kinematic calibration of robots containing closed loops, J. Mech. Des. 125(1) (2003) 23–32.
[20] R. He, Y. Zhao, S. Yang, S. Yang, Kinematic-parameter identification for serial-robot calibration based on POE formula, IEEE Trans. Robot. 26(3) (2010) 411–423.
[21] X. Yang, L. Wu, J. Li, K. Chen, A minimal kinematic model for serial robot calibration using POE formula, Robot. Comput. Integr. Manuf. 30(3) (2014) 326–334.
[22] Y. Lou, T. Chen, Y. Wu, Z. Li, S. Jiang, Improved and modified geometric formulation of POE based kinematic calibration of serial robots, in: Proc. 2009 IEEE/RSJ Int. Conf. Intell. Robot. Syst., St. Louis, MO, USA, (2009) 5261–5266.
[23] Y. Wu, C. Li, J. Li, Z. Li, Comparative study of robot kinematic calibration algorithms using a unified geometric framework, in: Proc. 2014 IEEE Int. Conf. Robot. Autom., Hong Kong, China, (2014) 1393–1398.
[24] G. Chen, H. Wang, Z. Lin, Determination of the identifiable parameters in robot calibration based on the POE formula, IEEE Trans. Robot. 30(5) (2014) 1066–1077.
[25] C. Li, Y. Wu, H. Löwe, Z. Li, POE-Based robot kinematic calibration using axis configuration space and the adjoint error model, IEEE Trans. Robot. 32(5) (2016) 1264–1279.
[26] L. Wu, X. Yang, K. Chen, H. Ren, A minimal POE-based model for robotic kinematic calibration with only position measurements, IEEE Trans. Autom. Sci. Eng. 12(2) (2015) 758–763.
[27] A. Pashkevich, Computer-aided generation of complete irreducible models for robot manipulators, in: Int. Conf. Model. Simul., Troyes, France, (2001) 293-298.
[28] T. Huang, D. Zhao, F. Yin, W. Tian, D.G. Chetwynd, Kinematic calibration of a 6-DOF hybrid robot by considering multicollinearity in the identification Jacobian, Mech. Mach. Theory 131 (2019) 371–384.
[29] S. Besnard, W. Khalil, Identifiable parameters for parallel robots kinematic calibration, in: Proc. 2001 IEEE Int. Conf. Robot. Autom., Seoul, South Korea, (2001) 2859–2866.
[30] P. Huang, J. Wang, L. Wang, R. Yao, Identification of structure errors of 3-PRS-XY mechanism with regularization method, Mech. Mach. Theory 46(7) (2011) 927–944.
[31] Y. Liu, J. Wu, L. Wang, J. Wang, Parameter identification algorithm of kinematic calibration in parallel manipulators, Adv. Mech. Eng. 8(9) (2016) 1–16.
[32] Y. Hu, F. Gao, X. Zhao, B. Wei, D. Zhao, Y. Zhao, Kinematic calibration of a 6-DOF parallel manipulator based on identifiable parameters separation (IPS), Mech. Mach. Theory 126 (2018) 61–78.
[33] L. Kong, G. Chen, Z. Zhang, H. Wang, Kinematic calibration and investigation of the influence of universal joint errors on accuracy improvement for a 3-DOF parallel manipulator, Robot. Comput. -Integr. Manuf. 49 (2018) 388–397.
[34] G. Xiong, Y. Ding, L. Zhu, A product-of-exponential-based robot calibration method with optimal measurement configurations, Int. J. Adv. Robot. Syst. 14(6) (2017) 1–12.
[35] A. Klimchik, S. Caro, B. Furet, A. Pashkevich, Practically identifiable model of robotic manipulator for calibration in real industrial environment. In: E. Menegatti, N. Michael, K. Berns, H. Yamaguchi (Eds.), Intelligent Autonomous Systems 13, Springer, Cham, Switzerland, (2016) 675-689.
[36] A. Klimchik, S. Caro, A. Pashkevich, Optimal pose selection for calibration of planar anthropomorphic manipulators, Precis. Eng. 40 (2015) 214–229.
[37] C. Lin, Kinematic calibration for closed loop robots, Ph.D. Thesis, Texas A&M University, (1990).
[38] P. Vischer, Improving the accuracy of parallel robots, Ph.D. Thesis, Ecole Polytechnique Fédérale De Lausanne, (1996).
[39] G. Legnani, D. Tosi, R. Adamini, I. Fassi, Calibration of parallel kinematic machines: theory and applications, in: K.H. Low (Ed.), Industrial Robotics: Programming, Simulation and Applications, Verlag, Mammendorf, Germany, (2006) 171–194.
[40] G. Chen, L. Kong, Q. Li, H. Wang, Z. Lin, Complete, minimal and continuous error models for the kinematic calibration of parallel manipulators based on POE formula, Mech. Mach. Theory 121 (2018) 844–856.
[41] H. Liu, T. Huang, D.G. Chetwynd, A general approach for geometric error modeling of lower mobility parallel manipulators, J. Mech. Robot. 3(2) (2011) 021013.1–13.
[42] J. Dai, Z. Huang, H. Lipkin, Mobility of overconstrained parallel mechanisms, J. Mech. Des. 128(1) (2006) 220-229.
[43] J. Dai, J.R. Jones, Interrelationship between screw systems and corresponding reciprocal systems and applications, Mech. Mach. Theory 36(5) (2001) 633–651.
[44] T. Huang, S. Yang, M. Wang, T. Sun, D.G. Chetwynd, An approach to determining the unknown twist/wrench subspaces of lower mobility serial kinematic chains, J. Mech. Robot. 7(3) (2015) 031003.1–9.